JCTC Journal of Chemical Theory and Computation

Article

pubs.acs.org/JCTC

TD-DFT Assessment of Functionals for Optical 0−0 Transitions in Solvated Dyes

Denis Jacquemin,*[,†] Aurélien Planchat,[†] Carlo Adamo,*[,‡,§] and Benedetta Mennucci*[,∥]

[†]Laboratoire CEISAM-UMR CNR 6230, Université de Nantes, 2 Rue de la Houssinière, BP 92208, 44322 Nantes Cedex 3, France

[‡]Laboratoire LECIME, CNRS UMR-7575, Chimie-ParisTech, 11 rue Pierre et Marie Curie, F-75231 Paris Cedex 05 France

[§]Institut Universitaire de France, 103 bd Saint-Michel, F-75005 Paris Cedex 05, France

[∥]Department of Chemistry, University of Pisa, Via Risorgimento 35, 56126 Pisa, Italy

Supporting Information

ABSTRACT: Using TD-DFT, we performed simulations of the adiabatic energies of 40 fluorescent molecules for which the experimental 0−0 energies in condensed phase are available. We used six hybrid functionals (B3LYP, PBE0, M06, M06-2X, CAM-B3LYP, and LC-PBE) that have been shown to provide accurate transition energies in previous TD-DFT assessments, selected two diffuse-containing basis sets, and applied the most recent models for estimating bulk solvation effects. In each case, the correction arising from the difference of zero-point vibrational energies between the ground and the excited states has been consistently determined. Basis set effects have also been carefully studied. It turned out that PBE0 and M06 are the most effective functionals in terms of average deviation (mean absolute error of 0.22−0.23 eV). However, both the M06-2X global hybrid that contains more *exact* exchange and the CAM-B3LYP range-separated hybrid significantly improve the consistency of the prediction for a relatively negligible degradation of the average error. In addition, we assessed (1) the cross-structure/spectra relationships, (2) the importance of solvent effects, and (3) the differences between adiabatic and vertical energies.

1. INTRODUCTION

Density functional theory (DFT) is certainly the most widely used ab initio approach in both organic and inorganic chemistry. This success can be traced back to the beginning of the 1990s, in particular, to 1993, with the seminal works of Becke proposing to create hybrid functionals that mix DFT exchange (and correlation) with *exact* exchange of Hartree−Fock (HF) form.[1,2] The B3LYP functional, which contains 20% of HF-like exchange, has allowed impressive improvements of the predictions of computational chemistry for a rather modest increase of the computational cost. Of course, since this breakthrough, significant advances have been achieved in order to provide more accurate and more refined functionals. Notably, ab initio functionals that are free of fitted parameters and/or methods showing a broader range of applicability,[3−8] hybrid functionals dedicated to investigation of transition states and kinetics,[7−9] range-separated hybrids (RSH) that allow one to accurately simulate charge-transfer states as well as nonlinear optical properties,[10−15] double-hybrid functionals that explicitly depend on the virtual orbitals,[16−21] and dispersion-corrected approaches that paved the way toward the calculation of weak interactions,[22−26] have all contributed to the successes of DFT.

Extension of DFT to electronically excited states, namely, time-dependent density functional theory (TD-DFT), was proposed more than 25 years ago[27−32] and stands, as its ground-state (GS) counterpart, as the most widely used theoretical approach to compute the transition energies to the electronically excited state (ES) as well as to evaluate related properties (ES dipole, geometries, densities, ...). TD-DFT tends to significantly outperform simpler theories (ZINDO/S, PM6, CIS, ...)[33−35] while remaining much more affordable than the electron-correlated wave function approaches, namely, EOM-CC,[36] CAS-PT2,[37] SAC-CI,[38,39] and MR-CI.[40] As it is well recognized that ES properties are environmentally sensitive, it should also be pointed out that the development and implementations of approaches, allowing one to consistently model solvatochromic effects during TD-DFT simulations, is an extra clear-cut advantage.[41−45] Despite its successes and versatility, TD-DFT suffers from, at least, a major practical limitation: the reliability of the results depends significantly on the selected exchange-correlation (xc) functional. If chemical accuracy (ca. 0.10 eV) may not yet been reached on a systematic basis, this might be partially explained: the vast majority of functionals have been developed, parametrized, and optimized for GS properties. As the potential energy surfaces of the ES tend to be significantly flatter than their GS counterparts, this limitation might have a significant incidence. For instance, it has been demonstrated that accurately quantifying the relative importance of twisted and planar intramolecular charge transfer states is an impossible task for traditional xc functionals. Indeed, typical hybrids like B3LYP and PBE0 provide reasonable estimates of the geometrical parameters of the GS but qualitatively fail for the ES as they foresee a fully twisted donor group, a prediction negated by accurate wave function approaches or RSH.[46−48] Of course, as today's implementation relies on a single determinant, TD-DFT is inadequate when multiple states are energetically close, e.g., when a conical intersection between the GS and the ES plays a key role or when the ES cannot be described in terms of

Received: April 26, 2012
Published: June 4, 2012

single excitation. In these cases, only multireference methods may provide an accurate description of the excited-state properties.

In that framework, benchmarking DFT functionals for TD-DFT applications is of crucial importance in order to produce accurate or, at least, chemically sound results. Three years ago, we published an extensive TD-DFT investigation,[49] and earlier benchmark works are summarized in Table 1 of this work. Since that time, several significant TD-DFT assessments have appeared in the literature.[50−65] Though the results of these previous works are certainly not uniform, a general conclusion emerged: xc functionals that do not include HF exchange (that is, *pure* or nonhybrid functionals) provide poor estimates as they tend to severely undershoot the transition energies. In 2009, we performed vertical TD-DFT calculations,[49] i.e., we used optimal GS structures to perform single-point TD-DFT calculations ($E^{\text{vert-a}}$ in Figure 1). One can consistently compare these values with the results of high-level wave function vertical simulations performed with the very same protocol, e.g., one can rely on Thiel's CAS-PT2/CC3 benchmark set,[66−70] though these wave function data cannot be viewed as error free.[71,72] However, confronting vertical TD-DFT figures to the experimental wavelength of maximal absorption (λ_{max}) is a not a completely satisfying approach, despite the huge popularity of this approximation. Indeed, a more physically sound reference is the 0−0 energy, that is, the difference of GS and ES energies obtained at their respective minimum (E^{adia}) and corrected for the difference of zero-point vibrational energy (ZPVE) between the GS and the ES (see Figure 1). Determination of E^{0-0} implies at least three difficulties: (1) one needs to calculate the ZPVE of the ES, and thus the ES Hessian, a Dantean numerical task for nonsymmetric molecules encompassing more than 25 atoms, (2) the environmental effects distinctly tune the GS and ES properties and cannot be straightforwardly computed (see section 2.4), and (3) while one can find a profusion of experimental λ_{max} in the literature, accurate 0−0 values are rather uncommon.

Table 1. Experimental Values Used as Reference in This Study (in eV)[a]

molecule	solvent	λ_{max}	0−0	ref
I	cyclohexane	5.02	4.56	97
II	methanol	2.49	2.48	111
III	water	3.82	3.46	94
IV	hexane	3.92	3.50	98
V	ethanol	3.35	2.98	92
VI	dioxane	3.77	3.53	108
VII	benzene	3.25	2.92	116
VIII	cyclohexane	1.93	1.89	118
IX	ethanol	3.14	3.10	91
X	benzene	2.87	2.85	91
XI	dichloromethane	1.97	1.95	97
XII	2-methylbutane	3.42	3.18	114
XIII	cyclohexane	2.99	2.76	112
XIV	cyclohexane	3.55	3.11	106
XV	dichloromethane	3.09	2.85	115
XVI	toluene	2.78	2.30	119
XVII	ethanol	2.70	2.53	97
XVIII	dichloromethane	2.00	1.95	120
XIX	ethanol	2.27	2.18	91
XX	benzene	2.50	2.29	91
XXI	chloroform	3.50	3.29	102
XXII	ethyl acetate	2.91	2.66	121
XXIII	acetonitrile	3.32	2.99	122
XXIV	2-methylbutane	3.16	2.98	99
XXV	chloroform	1.73	1.71	110
XXVI	ethanol	2.07	2.02	93
XXVII	chloroform	3.37	3.15	101
XXVIII	dimethylformamide	2.37	2.33	124
XXIX	dichloromethane	2.51	2.24	123
XXX	ethanol	3.01	2.65	103
XXXI	dioxane	2.18	2.12	105
XXXII	dichloromethane	3.57	3.25	107
XXXIII	water	2.78	2.40	113
XXXIV	acetontrile	2.97	2.76	117
XXXV	carbontetrachloride	2.47	2.28	96
XXXVI	hexane	3.21	2.72	109
XXXVII	ethanol	4.01	3.88	97
XXXVIII	toluene	2.91	2.64	104
XXXIX	dimethylformamide	3.33	2.76	100
XL	toluene	1.85	1.83	95

[a]Molecules are depicted in Schemes 1 and 2. The 0−0 energies are the crossing point between the absorption and fluorescence curves (see Introduction). λ_{max} corresponds to the longest wavelength of absorption maxima (in eV). When a clear vibrational pattern is present, λ_{max} has been selected as the strongest absorbing peak, consistently with ref 49.

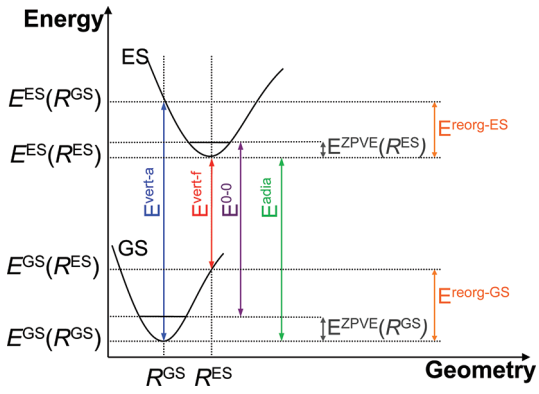

Figure 1. Representation of the main parameters computed.

In the framework of adiabatic TD-DFT benchmarks, two works undoubtedly deserve to be highlighted. On one hand, Furche and co-workers[58] collated a large (109 cases) set of accurate experimental adiabatic energies of gas-hase molecules. This choice circumvents the above-mentioned second difficulty, whereas the impact of the third problem is to confine the set to small molecules (but for a few exceptions, e.g., porphyrin). In ref 58 the authors computed the ZPVE corrections with the B3LYP functional and adjusted the results of the other tested functionals (namely, LSDA, PBE, BP86, TPSS, and PBE0) with the B3LYP vibrational correction. For a subset of compounds, they showed that the difference between B3LYP and PBE0 ZPVE corrections was very small. Furche's work is therefore complete for small gas-phase molecules, though only two traditional xc hybrids have been benchmarked. On the other hand, Goerigk and Grimme performed TD-DFT benchmarks for 5[50] and then 12[51] large solvated dyes. They used the crossing point of the measured fluorescence and absorption bands as experimental 0−0 reference, a choice that we follow in the present contribution. To partly bypass both the first and the second complications, they applied a smart modus operandi:

Scheme 1. Representation of the First Series of Compounds Investigated Herein

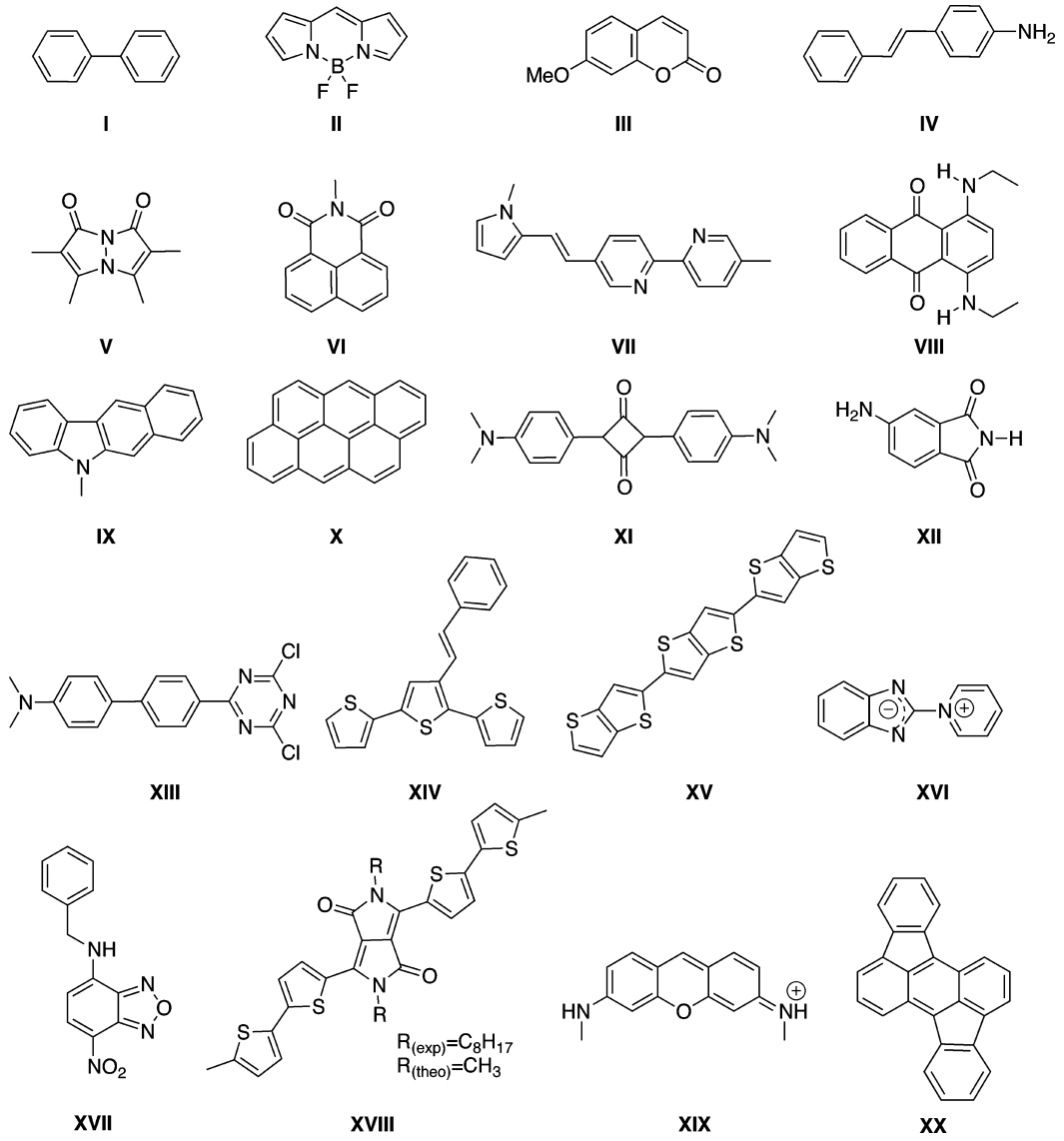

transformation of these experimental 0−0 data in vertical values thanks to application of successive theoretical corrections. Indeed, Goerigk and Grimme first performed standard nonequilibrium linear-response polarizable continuum model calculations (PCM,[73] see section 2.4) to remove solvent effects. Next, they computed the ZPVE GS-ES shift as well as the difference between the adiabatic and the vertical absorption energies, both at the PBE/TZVP level, to obtain "experimental" vertical energies. They considered these estimates to be accurate within a ±0.1 eV threshold. This allowed the use of vertical TD-DFT calculations to assess xc functionals. Despite these previous efforts, more is needed to assess the relative accuracy of TD-DFT functionals for "real-life" conjugated molecules. Here, we propose for the first time a modeling of 0−0 energies accounting for both ZPVE and solvent effects in a fully consistent way: both the GS and the ES geometries of each compound have been optimized and vibrationally characterized for all functionals with a systematic inclusion of bulk solvent effects with the PCM model. In addition, we go beyond the linear-response PCM approximation. Though this is certainly not the end of the (in)famous "what is the best TD functional" controversy, we are convinced that the present contribution represents a significant step to shed a extra light into this debate, as we avoid most simplifications in our assessment.

2. METHODOLOGY

2.1. Computational Details. All calculations have been performed with the Gaussian09.A02 revision[74] except for computation of fluorescence wavelengths that have been performed with a locally modified version of the same code. We used six functionals, B3LYP,[2,75] PBE0,[4,5] M06,[8] M06-2X,[8] CAM-B3LYP[12] and LC-PBE,[11,76] that have been shown to be promising in previous benchmarks.[49,51,53,54,56,64,77−80] We redirect interested readers to these original references for more details about the mathematical form of these six hybrids. Nevertheless, let us point out that the selected LC-PBE implementation uses an attenuation parameter of 0.47 that corresponds to the 2007 parametrization[76] rather than the original 0.33 value of 2001.[11] After extensive atomic basis set (BS) assessment (see section 3.1), we mainly relied on the 6-31+G(d) and 6-311++G(d,p) BS, denoted A and B in the

Scheme 2. Representation of the Second Series of Compounds Investigated Herein

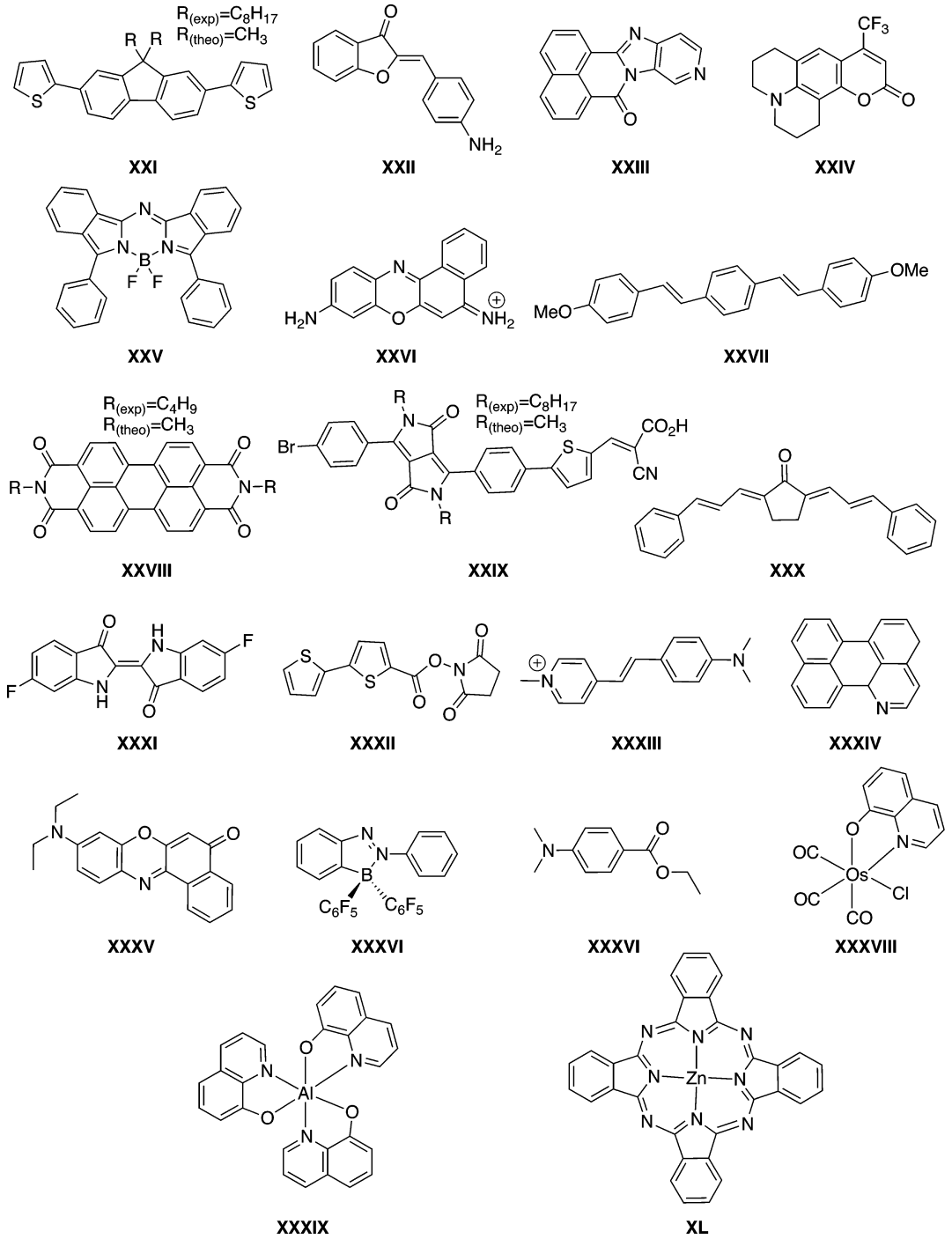

following. Indeed, they yield nearly perfectly converged results for most parameters of interest. The 6-311++G(2df,2p) basis set (C) has also been used to perform corrections on the vertical transition energies (see section 2.4). In Gaussian09, the A BS uses *6d* functions whereas the B and C BS rely on *5d* functions, and we followed this default. The osmium (**XXXVIII**) and zinc (**XL**) atoms have been modeled with the LanL2DZ basis set and pseudopotential.[81,82] There are no significant effects of the selected pseudopotential for optical transitions in this kind of complexes.[83] In the vast majority of our calculations we used the Euler−Maclaurin integration "fine" grid constituted of 75 radial and 302 angular points. In the few cases where convergence could not be achieved with this "fine" grid, a tighter (99 590) grid has been applied. Of course, for a given case, the same grid was systematically used for both the GS and the ES. Wheeler and Houk carefully investigated the relationship between the size of the integration grid and the obtained results for the M06 functional family,[84] and their results showed that the (75 302) grid generally produces very small errors compared to much larger grids for both M06 and M06-2X (mean absolute deviation of ca. 0.02 kcal/mol for reaction energies). The GS and ES geometries have been determined with the Berny-GEDIIS algorithm[85] using a 1×10^{-5} au threshold for the rms force (tight keyword in

dx.doi.org/10.1021/ct300326f | J. Chem. Theory Comput. 2012, 8, 2359−2372

Gaussian). To ensure valid description of the geometric and vibrational features, we also used an energy convergence threshold of at least 1×10^{-9} au. Force minimizations have been performed thanks to the analytical DFT and TD-DFT gradients available for the ground and excited states, respectively.[43,86−88] When several chemically sound conformers could be designed, they have been first considered and only the most stable GS structures are reported. The GS and ES vibrational frequencies have been computed using analytical and numerical derivatives, respectively. Given the size of most investigated molecules, the latter step was by far the most time consuming. We roughly estimate that ca. 400 years of (single-core) CPU time were needed to achieve all calculations and that ca. 90% of that time was devoted to determination of the ZPVE corrections of the ES. Apart from allowing one to compute the ZPVE, these vibrational calculations allowed us to ascertain that both the GS and the ES geometries are true minima of the potential energy surface. When symmetry operations could be foreseen, the highest possible point group was initially enforced and (possibly) progressively degraded if imaginary frequencies were found. For modeling solvent effects, we used the well-known PCM scheme,[73] which allows one to account for bulk solvation effects. PCM splits the problem into a solute (the chromogen) that is inside a cavity surrounded by a structureless media that has the macroscopic characteristics of the solvent. We selected (see section 2.4) a panel of PCM models for computing the transition energies. For both GS and ES calculations we used the same cavities obtained by selecting the G09 defaults (vdW cavities based on UFF radii scaled by 1.1).There is in fact no clear evidence that ES cavities should be different from GS ones, and we believe that the parameters used here are sufficiently general to be properly applied to both ground and excited states. For a more detailed discussion of the relationship between the PCM parameters and the computed ES properties we redirect the interested readers to previous investigations.[89,90]

2.2. Benchmark Set. Experimental values have been collected in Table 1,[91−124] whereas the molecules used in our benchmarks are displayed in Schemes 1 and 2. For the former set we used both A and B basis sets, whereas for the latter only the A BS has been used. Compared to the experimentally characterized compounds, we performed no structural simplification except for the long butyl and octyl chains that have been replaced by methyl groups in four cases (**XVII**, **XXI**, **XXVIII**, and **XXIX**). This substitution should have only a trifling impact on the optical properties.

The molecules under investigation are representative of conjugated dyes. Though we certainly do not wish to perform a full review of previous works on all molecules, we emphasize that our set encompasses the most important industrial fluorophores, namely, coumarins (**III** and **XXIV**), which have been the subject of numerous previous TD-DFT investigations,[125−131] naphthalimides and related cousins (**VI**, **XII**, and **XXVIII**), which have also been the focus of other modeling works,[132−136] and (aza-)BODIPY (**II** and **XXV**), which are known to be difficult to model with standard theoretical approaches.[137−139] Additionally, a special effort has been done to include recently synthesized/characterized molecules (e.g., **XVI**, **XVIII**, **XXII**, ...)[118−124] as well as cyanine-like derivatives (**XIX** and **XXXIII**). This latter group has attracted intense discussion regarding the accuracy of TD-DFT.[49,71,72,140,141] It turns out that previously encountered problems in cyanines are mainly related to the selection of the vertical approximation (we redirect the interest reader to ref 72 for more a complete discussion), in other words the selected reference value is of high importance for these dyes. Our set also includes a molecule that has demonstrated interesting features for dye-sensitized solar cell applications,[123] namely, **XXIX**, and three inorganic compounds, **XXXVIII**, **XXXIX**, and **XL**. Note that 11 out of the 12 molecules of Grimme's set[51] are included in the present work (computation of the ZPVE correction of the last molecule being beyond computational reach).

As mentioned in the Introduction, the principal limit of our benchmark set is the availability of experimental values, for which we have been confronted with the same problem as Furche for his small gas-phase molecule set.[58] In that framework, it is clear that only molecules presenting a non-negligible fluorescence yield could be benchmarked. Indeed, we have mainly conjugated and delocalized compounds in our set. Though this means that the conclusion obtained here might not be completely transferrable to different cases (e.g., a heavy-atom metallic dimer) this restriction is not too bothering: most people performing TD-DFT simulations or interested in analysis of experimental optical spectra are tackling similar conjugated derivatives. Therefore, while we do not oversee all chemistry, our set is relevant of actually synthesized molecules for which optical simulations are done.

2.3. 0−0 Energies. The main data that are computed in this contribution are graphically summarized in Figure 1. We first discuss the simpler gas-phase situation. In that case, the vertical absorption corresponds to the difference of the GS and ES energies computed for the GS optimal geometries, that is

$$E^{\text{vert-a}} = E^{\text{ES}}(R^{\text{GS}}) - E^{\text{GS}}(R^{\text{GS}}) \tag{1}$$

and the vertical fluorescence is the corresponding value estimated for the ES structure

$$E^{\text{vert-f}} = E^{\text{ES}}(R^{\text{ES}}) - E^{\text{GS}}(R^{\text{GS}}) \tag{2}$$

These two transition energies are readily given by most computational programs, the former by a single-point TD-DFT calculation performed on the GS geometries and the latter being the TD-DFT energy obtained at the end of an ES TD-DFT geometry optimization. The adiabatic energy is the difference of total electronic energies computed for the ES and GS in their corresponding optimal geometries

$$E^{\text{adia}} = E^{\text{ES}}(R^{\text{ES}}) - E^{\text{GS}}(R^{\text{GS}}) \tag{3}$$

There is an alternative way to define this energy by combining the vertical absorption and fluorescence data to the ES and GS reorganization energies (see Figure 1). Indeed, from eq 3, one gets

$$E^{\text{adia}} = E^{\text{ES}}(R^{\text{ES}}) - E^{\text{GS}}(R^{\text{GS}}) \tag{4}$$

$$= E^{\text{vert-f}} + E^{\text{GS}}(R^{\text{ES}}) - E^{\text{ES}}(R^{\text{GS}}) + E^{\text{vert-a}} \tag{5}$$

$$= E^{\text{vert-f}} + E^{\text{vert-a}} + E^{\text{GS}}(R^{\text{ES}}) + E^{\text{reorg-GS}} - E^{\text{ES}}(R^{\text{ES}}) - E^{\text{reorg-ES}} \tag{6}$$

$$= E^{\text{vert-f}} + E^{\text{vert-a}} + E^{\text{adia}} + E^{\text{reorg-GS}} - E^{\text{reorg-GS}} \tag{7}$$

and hence

$$E^{\text{adia}} = \frac{1}{2}[E^{\text{vert-f}} + E^{\text{vert-a}}] + \frac{1}{2}[E^{\text{reorg-GS}} - E^{\text{reorg-ES}}] \tag{8}$$

In a first crude approximation one can neglect the second term

$$E^{adia} \simeq \frac{1}{2}[E^{vert\text{-}f} + E^{vert\text{-}a}] \quad (9)$$

In addition, there is a variation of the zero-point vibrational energy (ZPVE) between the GS and the ES

$$\Delta E^{ZPVE} = E^{ZPVE}(R^{GS}) - E^{ZPVE}(R^{ES}) \quad (10)$$

a parameter that is almost systematically positive as the excited-state potential energy surfaces tend to be flatter than their GS counterparts. As discussed above, computing this term requires determination of the Hessian of the ES, a task that can only be performed numerically at the (PCM-)TD-DFT level to date.[43] Once ΔE^{ZPVE} is known, the 0−0 energy simply becomes

$$E^{0-0} = E^{adia} - \Delta E^{ZPVE} \quad (11)$$

For comparison with experimental 0−0 points, this last parameter is meaningful provided the experiments are carried out in the gas phase, which is almost never the case for "real-life" fluorophores of industrial interest.

2.4. Solvent Effects. In solution, one should distinguish two mechanisms of solute−solvent interactions for ES phenomena, namely, the equilibrium (eq) and nonequilibrium (neq) modes. In the former, the solvent polarization has time to fully adapt to the new electronic configuration of the solute and the effective dielectric constant used in the calculation is the static limit (e.g., 46.7 for DMSO). In the latter, only the electronic component of the solvent polarization has time to react (fast component) and the effective dielectric constant is ε_∞ (ca. 2 for most solvent). Clearly, while the ES geometry optimizations have to be performed in the equilibrium approach, the measured absorption and fluorescence bands are better corresponding to the nonequilibrium limit. We also note that this partition into fast and slow components of the solvent polarization does not apply to apolar solvents for which $\varepsilon = \varepsilon_\infty$.

To estimate the transition energies, several PCM models are available, namely, the classical linear-response (LR),[41,142] the corrected linear-response (cLR),[42] the vertical excitation model (VEM),[45] and the state-specific (SS) approximations.[128] The three latter more accurate and physically sound approaches take into account the variations of the polarization of the solvent following the electronic density rearrangements of the solute. It is our experience that the differences between the LR and the cLR transition wavelengths might be significant (see Supporting Information and section 3.3), whereas the VEM−cLR and SS−cLR discrepancies are generally modest, and we therefore selected the cLR scheme for our calculations as it is significantly less time consuming.[143]

In addition, for solvated systems, as previously shown for the gas phase, E^{adia} can be either calculated using eqs 3 and 8 or estimated in terms of the approximated eq 9. Now, however, we have to properly account for the possible nonequilibrium effects.

In the case of apolar solvents, for which this further aspect of nonequilibrium solvation does not play a role, exactly the same equations defined for the gas-phase systems apply. In practice, $E^{ES}(R^{ES})$ and $E^{vert\text{-}f}$ are directly obtained from the same fluorescence calculations and $E^{GS}(R^{GS})$ and $E^{vert\text{-}a}$ from the same absorption calculations, in both cases using the cLR model. From the resulting E^{adia}(cLR) values, 0−0 energies are finally obtained by subtracting the ΔE^{ZPVE} correction, which is here determined in the equilibrium limit of the LR version of PCM. In other words, for apolar solvent, one can apply

$$E^{0-0}(cLR) = E^{adia}(cLR) - \Delta E^{ZPVE}(LR) = E^{ES}(R^{ES}, cLR) - E^{GS}(R^{GS}) - \Delta E^{ZPVE}(LR) \quad (12)$$

To have an idea of the impact of the reorganization energies in eq 8, we compared the results of the exact eq 12 to the approximated

$$E^{0-0}(cLR) \simeq \frac{1}{2}[E^{vert\text{-}f}(cLR) + E^{vert\text{-}a}(cLR)] - \Delta E^{ZPVE}(LR) \quad (13)$$

for the 17 molecules in apolar solvents and 6 functionals (with the A basis set). The resulting mean absolute deviation obtained is limited to 0.018 eV, basically 1 order of magnitude below the investigated functional effects. When moving to polar solvents, the nonequilibrium effects lead to a correction of the positions of the absorption/fluorescence bands

$$\Delta E^{vert\text{-}x} = E^{vert\text{-}x}(cLR, neq) - E^{vert\text{-}x}(cLR, eq) \quad (14)$$

where -x is -a for absorption and -f for fluorescence. Having determined these two corrections, one can compute a nonequilibrium-corrected 0−0 energy as

$$E^{0-0}(cLR, neq) = E^{0-0}(cLR, eq) + \frac{1}{2}[\Delta E^{vert\text{-}a} + \Delta E^{vert\text{-}f}] \quad (15)$$

where the one-half factor is readily explainable from eq 8 and E^{0-0}(cLR,eq) is computed through eq 12. It is important to stress that this term is not the adiabatic energy (which should be computed in equilibrium irrespective of the solvent) but is the most relevant theoretical estimate of the crossing point between the absorption and the fluorescence curves.

To finally account for the (rather small) impact of BS effects, E^{0-0}(LR,eq) have been calculated with both the A and the B BS for the 20 molecules of Scheme 1. Additionally, the vertical absorption energies have been computed with both the C and the A BS using A geometries in order to yield our theoretical best estimate (TBE)

$$E^{0-0}(TBE) = E_A^{0-0}(cLR, neq) + [E_C^{vert\text{-}a}(LR, neq) - E_A^{vert\text{-}a}(LR, neq)] \quad (16)$$

where the subscripts indicate the selected atomic basis set. Despite its refinement, this procedure is not flawless. As the BS effects are well under control (see below), the main limitations of the TBE are, on the one hand, the lack of explicit solute−solvent interactions in the PCM model and, on the other hand, the inherent limit of choosing the absorption/emission crossing point as reference. For the first limit, we selected, when possible, apolar and aprotic media, but several experiments are unfortunately only available in alcohols or even water. For the second point, this choice as 0−0 reference implies that the absorption and fluorescence curves are perfectly symmetric, which is not systematically true for the 40 chromophores under investigation. In the Supporting Information, two (more approximated) alternatives to reach the TBE are presented (section S4) for interested readers.

3. RESULTS

3.1. Basis Set Effects. Of course, any benchmarking of DFT functionals must rely on basis sets yielding converged

results or at least providing errors much smaller than the typical experiment/theory variations under study. We therefore used several members of Pople's,[144−146] Dunning's,[147−149] and Jensen's[150−152] BS series, incorporating or not diffuse orbitals, to ascertain the quality of the A and B BS. Table 2 reports the vertical absorption and adiabatic energies as well as the difference of ZPVE between the GS and the ES for the first three molecules of Scheme 1. These compounds are rather small, allowing extensive BS evaluation. In addition, these dyes represent a valuable panel of chemical cases. Indeed, the aromatic biphenyl (**I**) undergoes a strong deformation from a distorted GS to an almost flat ES, the BODIPY core (**II**) is known to be a challenging cyanine-like molecule with a small Stokes shift, whereas the 7-OMe-coumarin (**III**) is a prototypical large-Stokes fluorophore possessing a rather localized excited state. For coumarins, the structural deformation induced by the electronic transition depends significantly on the selected method.[129]

Among all tested BS, *aug*-cc-pVTZ is the largest and has been selected as reference, a typical choice for TD-DFT works (note that *aug*-pc-2 calculations have been attempted but fail to properly converge). For the time-limiting ΔE^{ZPVE}(LR,eq) step, one notices that the BS effects are trifling. In fact, provided a BS with an adequate balance between polarization and diffuse functions is selected, the BS-related variations are one order of magnitude smaller than the changes induced by the functional. Indeed, the latter are typically of the order of 0.010−0.020 eV for the PBE0/CAM-B3LYP pair (see also section 3.2), whereas the difference between the 6-31+G(d) and the *aug*-cc-pVTZ ΔE^{ZPVE}(LR,eq) results is at most 0.004 eV. For **I**, use of diffuse-free triple-ζ BS, e.g., cc-pVTZ, pc-2, or 6-311G(d,p), yields errors of ca. 0.010 eV, and these BS are less satisfying than the more compact 6-31+G(d). For **II** and **III** one could go toward any BS choice and still reach sound ΔE^{ZPVE}(LR,eq) estimates. The same trends have been reported for one anthraquinone[59] and three bicylic chromogens.[65] Therefore, even a simple and quick 6-31G calculation could provide the vibrational correction to the adiabatic energies with sufficient accuracy to benchmark DFT functionals. However, it should not be inferred that such tiny BS is adequate for investigating other properties related to the vibrational signatures, e.g., 6-31G vibronic shapes are far from satisfying.[59]

For the vertical absorption energies, we observe the expected BS trends: (1) addition of diffuse orbitals is mandatory and tends to decrease the transition energies, (2) going from a double-ζ to a triple-ζ BS induces rather small variations, (3) including additional polarization orbitals tends to slightly decrease $E^{vert\text{-}a}$, and (4) BS effects are nearly independent of the selected functional. This latter statement can be illustrated by comparing the 6-31+G(d) and pc-1 energies to their *aug*-cc-pVTZ counterparts for **I**: the shifts are −0.042 and −0.157 eV (PBE0) or −0.033 and −0.150 eV (CAM-B3LYP), respectively. For **II** and **III**, both A and B basis sets yield values within 0.005 eV of the *aug*-cc-pVTZ reference, and this finding holds for E^{adia}. BS effects are larger for **I**, but it is noticeable that they are nearly parallel for $E^{vert\text{-}a}$(LR,neq) and E^{adia}(LR,eq). This suggests that the adiabatic energies can be corrected with the BS effects computed through vertical calculations: one can use a compact BS for the former and a larger one for the latter, as proposed by Grimme.[50,51] Performing this task for **I** with the A basis set provides a E^{adia}(LR,eq) best estimate of 4.314 (PBE0) and 4.446 eV (CAM-B3LYP),[153] very close to the corresponding *aug*-cc-pVTZ values of 4.311 and 4.439 eV, respectively.

Table 2. Influence of the Basis Set Choice on PCM-TD-DFT Transition Energies for Three Dyes: I, II, and III[a]

	I		II		III	
BS	PBE0	CAM-B3LYP	PBE0	CAM-B3LYP	PBE0	CAM-B3LYP
			$E^{vert\text{-}a}$(LR,neq)			
6-31G	5.161	5.429	3.129	3.129	4.087	4.339
6-31G(d)	5.076	5.347	3.127	3.084	4.142	4.375
6-311G(d,p)	5.021	5.298	3.088	3.046	4.117	4.345
6-31+G(d) [A]	4.946	5.204	3.048	2.999	4.059	4.279
6-311++G(d,p) [B]	4.938	5.204	3.040	2.993	4.057	4.279
6-311++G(2d,2p)	4.922	5.189	3.039	2.992	4.056	4.276
cc-pVDZ	5.007	5.268	3.085	3.042	4.104	4.329
cc-pVTZ	4.968	5.243	3.026	3.070	4.100	4.322
aug-cc-pVDZ	4.875	5.123	3.012	2.963	4.017	4.231
aug-cc-pVTZ	4.904	5.171	3.043	2.996	4.061	4.279
pc-0	5.127	5.408	3.156	3.139	4.096	4.361
pc-1	5.061	5.321	3.098	3.054	4.114	4.337
pc-2	4.936	5.209	3.057	3.010	4.084	4.305
aug-pc-0	5.104	5.386	3.050	3.023	3.997	4.248
aug-pc-1	4.956	5.213	3.033	2.981	4.057	4.267
			E^{adia}(LR,neq)			
6-31G	4.597	4.744	2.836	2.781	3.744	3.884
6-31G(d)	4.517	4.661	2.827	2.764	3.789	3.916
6-311G(d,p)	4.430	4.567	2.780	2.715	3.752	3.871
6-31+G(d) [A]	4.356	4.479	2.744	2.672	3.697	3.808
6-311++G(d,p) [B]	4.329	4.455	2.731	2.661	3.689	3.798
6-311++G(2d,2p)	4.317	4.444	2.732	2.662	3.690	3.797
cc-pVDZ	4.425	4.559	2.784	2.718	3.750	3.871
cc-pVTZ	4.385	4.519	2.764	2.696	3.735	3.848
aug-cc-pVDZ	4.276	4.394	2.709	2.634	3.659	3.765
aug-cc-pVTZ	4.311	4.439	2.736	2.666	3.696	3.803
pc-0	4.555	4.709	2.843	2.804	3.761	3.917
pc-1	4.415	4.544	2.786	2.720	3.748	3.878
pc-2	4.342	4.472	2.747	2.676	3.716	3.826
aug-pc-0	4.429	4.569	2.746	2.693	3.646	3.779
aug-pc-1	4.347	4.459	2.726	2.652	3.692	3.793
			ΔE^{ZPVE}(LR,eq)			
6-31G	0.132	0.128	0.099	0.078	0.116	0.108
6-31G(d)	0.129	0.123	0.098	0.073	0.116	0.107
6-311G(d,p)	0.131	0.125	0.096	0.070	0.116	0.107
6-31+G(d) [A]	0.121	0.112	0.098	0.073	0.116	0.107
6-311++G(d,p) [B]	0.123	0.114	0.097	0.072	0.118	0.109
6-311++G(2d,2p)	0.122	0.113	0.095	0.070	0.114	0.106
cc-pVDZ	0.128	0.116	0.096	0.070	0.114	0.105
cc-pVTZ	0.136	0.130	0.098	0.073	0.114	0.105
aug-cc-pVDZ	0.095	0.075	0.094	0.070	0.112	0.103
aug-cc-pVTZ	0.119	0.108	0.096	0.071	0.112	0.104
pc-0	0.121	0.111	0.100	0.075	0.120	0.110
pc-1	0.123	0.113	0.095	0.074	0.115	0.105
pc-2	0.128	0.118	0.097	0.072	0.115	0.106
aug-pc-0	0.096	0.086	0.098	0.074	0.116	0.106
aug-pc-1	0.151	0.136	0.091	0.070	0.123	0.110

[a]All values in eV. Selected solvents are cyclohexane (**I**), methanol (**II**), and water (**III**).

In short, the A BS is sufficient to estimate the properties under investigation in this work. Nevertheless, a small error on the vertical component could appear for specific cases and should not to be neglected. For this reason, we correct our 0–0 energies for BS effects, see eq 16. In addition, we computed the ΔE^{ZPVE}(LR,eq) of the first 20 molecules with the B BS to confirm our conclusions (see below and Supporting Information).

3.2. Theory–Experiment Comparisons. In Tables S-I and S-II in the Supporting Information, the reader can find a comparison between the E^{vert-a}(LR,neq), the ΔE^{ZPVE}(LR,eq), and the E^{0-0}(LR,eq) computed with the A and B basis sets for all molecules displayed in Scheme 1. For the 0–0 energies, the average impact of the BS is smaller than 0.01 eV for all functionals except for LC-PBE (0.02 eV), whereas the correlation coefficient between the results of the two BS exceeds 0.999 for all six hybrid functionals. Similarly, the average BS effect is smaller than 0.01 eV for ΔE^{ZPVE}(LR,eq), irrespective of the selected functional. This effect is slightly larger for the vertical transition energies, but as noted above, this is accounted for by the C BS corrections in our procedure. Therefore, we do not discuss further the values calculated with the B BS.

For all molecules and functionals, the computed TBE are listed in Table 3, whereas the full list of absorption, fluorescence, adiabatic, and vibrational energies can be found in the Supporting Information (Tables S-I–S-XV). Though it is not our goal to discuss the trends for each molecule, compound **XIII** is worth specific comment. Indeed, for this molecule the predicted ES geometry is strongly different for, on one hand, B3LYP and PBE0 and, on the other, M06-2X, CAM-B3LYP, and LC-PBE, M06 providing an intermediate situation. This is illustrated in Figure 2: while the GS structures are similar for all selected methods, B3LYP predicts a right angle between the rings at the ES minimum, contrary to the results obtained with M06-2X and, to a lesser extent, M06. This is one more illustration of the twisting problem of low-HF exchange hybrids (see Introduction). This fact was originally discussed by Tozer for a model push–pull molecule[46] and confirmed for larger structures afterward,[47,48] and it is clear that both B3LYP and PBE0 fail to provide a valid ES structure. Compound **XIII** is nevertheless slightly original, as the deformation does not occur only on the terminal diethylamino donor group but also on the vicinal phenyl ring. The functional dependencies shown in Figure 2 have important consequences, e.g., the oscillator strength corresponding to this emitting state is 0.0 for B3LYP, 0.74 for M06, and 1.52 with M06-2X. Interestingly, the very same molecule was pointed out to be problematic due to its charge-transfer nature by Goergik and Grimme.[51] As can be seen here, this charge-transfer "problem" goes beyond the topology of the orbitals associated to the transition. A similar difficulty can be pinpointed for the model betaine molecule, **XVI**, which has already been the subject of several joint theory/experiment works:[119,154,155] the first ES presents a trifling oscillator strength with B3LYP, PBE0, and M06 but large values with M06-2X, CAM-B3LYP, and LC-PBE. Despite these failures of hybrids incorporating 20–30% of HF exchange, we initially conserved them in our set as we wish to assess the features of each functional for 0–0 cases, and these qualitative deficiencies should be included.

In Table 4, we report the results of a statistical analysis—mean signed error (MSE), mean absolute error (MAE), root-mean-square deviation (rms), standard deviation (SD), linear correlation coefficient (R), as well as the maximal and the minimal deviations—obtained by comparing the TBE of Table 3 to the experimental values listed in Table 1. Figure 3 provides a graphical representation of the error patterns obtained for the six hybrid functionals. In the Supporting Information the results obtained with slightly less refined TBE models can be found in Tables S-XVI–S-XIX as well as in Figures S-1 and S-2. As they are qualitatively very similar, we do not discuss them further. The MSE is positive for B3LYP (i.e., the experimental values are underestimated), is close to zero for PBE0 and M06, and becomes significantly negative for the three remaining functionals; LC-PBE provides an average overestimation of 0.5 eV. At this exception, related to the very large attenuation parameter in LC-PBE, the MAE is similar for all selected functionals (0.22–0.26 eV), PBE0 providing the minimal

Table 3. Theoretical Best Estimates of the Experimental 0–0 Energies (in eV)[a]

molecule	B3LYP	PBE0	M06	M06-2X	CAM-B3LYP	LC-PBE
I	4.199	4.316	4.125	4.488	4.437	4.760
II	2.903	2.977	2.916	2.956	2.976	3.032
III	3.672	3.789	3.737	3.950	3.934	4.205
IV	3.227	3.315	3.210	3.497	3.504	3.803
V	2.941	3.083	3.103	3.259	3.260	3.612
VI	3.350	3.464	3.389	3.713	3.667	4.020
VII	2.766	2.865	2.813	3.081	3.125	3.471
VIII	1.986	2.045	2.073	2.245	2.243	2.481
IX	2.934	3.035	3.011	3.334	3.351	3.710
X	2.573	2.651	2.587	2.885	2.866	3.192
XI	2.295	2.362	2.335	2.403	2.416	2.535
XII	3.080	3.219	3.217	3.580	3.501	3.921
XIII	1.712	1.975	2.442	3.089	3.151	3.596
XIV	2.674	2.789	2.725	3.066	3.065	3.473
XV	2.499	2.622	2.566	2.875	2.850	3.285
XVI	1.629	1.808	1.773	2.515	2.486	3.306
XVII	2.586	2.772	2.726	3.034	2.992	3.377
XVIII	1.843	1.920	1.909	2.104	2.122	2.395
XIX	2.738	2.819	2.810	2.945	2.978	3.189
XX	2.030	2.108	2.071	2.349	2.353	2.687
XXI	2.961	3.083	3.004	3.384	3.359	3.747
XXII	2.707	2.816	2.833	3.089	3.125	3.413
XXIII	2.763	2.914	2.907	3.326	3.308	3.739
XXIV	2.769	2.925	2.948	3.316	3.294	3.667
XXV	1.898	1.931	1.872	1.968	1.972	2.005
XXVI	2.409	2.487	2.451	2.608	2.598	2.780
XXVII	2.716	2.808	2.722	3.070	3.098	3.475
XXVIII	2.154	2.232	2.213	2.461	2.441	2.775
XXIX	1.681	1.854	1.927	2.347	2.399	2.739
XXX	2.475	2.563	2.530	2.878	2.886	3.256
XXXI	2.064	2.218	2.263	2.480	2.478	2.770
XXXII	3.145	3.263	3.169	3.397	3.367	3.688
XXXIII	2.430	2.552	2.543	2.823	2.881	3.114
XXXIV	2.540	2.623	2.565	2.865	2.846	3.201
XXXV	2.430	2.511	2.492	2.711	2.704	2.973
XXXVI	2.329	2.443	2.454	2.972	2.907	3.235
XXXVII	3.831	3.960	3.926	4.222	4.221	4.520
XXXVIII	2.347	2.473	2.411	2.829	2.795	3.270
XXXIX	2.339	2.461	2.418	2.855	2.808	3.318
XL	1.918	1.954	1.873	1.945	1.888	1.646

[a]All values were obtained applying eq 16. Raw data are available in Supporting Information.

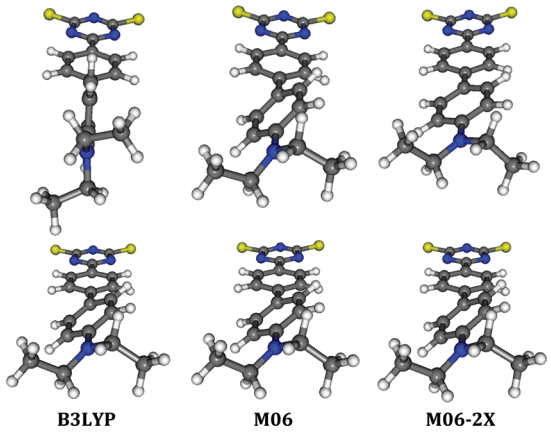

Figure 2. Perspective view of the optimal GS (bottom) and ES (top) geometries computed for molecule **XIII** using three different functionals (B3LYP, M06, and M06-2X).

Table 4. Statistical Analysis Obtained from Comparison of the Theoretical and the Experimental 0−0 Energies, Listed in Tables 3 and 1, Respectively (in eV)

method	MSE	MAE	rms	SD	*R*	max(+)	max(−)
B3LYP	0.14	0.27	0.33	0.21	0.86	0.56	−1.05
PBE0	0.03	0.22	0.28	0.17	0.89	0.64	−0.79
M06	0.05	0.23	0.27	0.15	0.89	0.63	−0.53
M06-2X	−0.25	0.26	0.31	0.18	0.95	0.77	−0.08
CAM-B3LYP	−0.24	0.25	0.31	0.18	0.94	0.80	−0.12
LC-PBE	−0.56	0.57	0.60	0.20	0.94	1.10	−0.18

deviation. The rms and SD display nearly the same evolutions as the MAE, though for these two criteria M06 has the edge. The maximal (positive and/or negative) deviations are large (typically >0.6 eV) for all functionals. By looking at the consistency of the prediction as measured by *R*, one notices that M06-2X, CAM-B3LYP, and LC-PBE clearly outperform B3LYP, PBE0, and M06. This point is also illustrated in Figure 3. Indeed, though PBE0 and M06 yield the smallest average deviation, M06-2X and CAM-B3LYP (which provide not only similar statistical data but also alike values for individual energies of the different dyes, see Supporting Information) are probably methods of choice when tackling 0−0 energies. This result is consistent with Grimme's analysis,[51] though details of the methodology significantly differ (see section 3.3 for further discussion). Eventually, we also performed a statistical analysis removing the two problematic dyes (**XIII** and **XVI**) as well as the three cationic structures (**XIX**, **XXVI**, and **XXXIII**) as the error patterns for neutral and charge structures could be significantly different.[49] For the remaining 35 compounds we obtained MAE of 0.23, 0.18, 0.20, 0.23, 0.22, and 0.52 eV for B3LYP, PBE0, M06, M06-2X, CAM-B3LYP, and LC-PBE, respectively. For the three first functionals, the *R* significantly improves (0.93−0.94). Therefore, removing the most "exotic" species diminishes the average errors without strongly affecting the relative performance of the tested functionals.

As can be seen in the Supporting Information, the ΔE^{ZPVE} contribution slightly varies with the selected functional but does not show any systematic behavior: ΔE^{ZPVE} increases or decreases with the amount of HF exchange depending on the molecule. In addition, the amplitude of the vibrational term is strongly related to the considered molecular structure. Consequently, computing the ZPVE with a given functional and applying the correction to other functionals[51,58] is a valid procedure. The ΔE^{ZPVE} term is generally within the 0.05−0.12 eV range and could be very roughly estimated as 0.08 eV when its computation is beyond reach because the molecules become too large. We emphasize that fully removing the ΔE^{ZPVE} from the benchmarks would significantly alter the conclusions. Indeed, the MAE determined in that way is 0.24, 0.33, and 0.32 eV for B3LYP, M06-2X, and CAM-B3LYP. In other words, omitting the ZPVE artificially improves (degrades) B3LYP (M06-2X and CAM-B3LYP) performance, a conclusion related to the sign of the MSE (Table 4). In the same vein, the PBE0 results, possessing a small positive MSE, are almost unaffected (statistically speaking) by the absence of the ZPVE correction: the MAE remains 0.22 eV.

3.3. Further Discussion. In this section we will answer three additional questions: (1) what is the relationship between the selected structure and the obtained spectral properties, (2) would a gas-phase approximation significantly affect the results, and (3) are benchmark conclusions conserved if one uses the usual vertical TD-DFT versus λ_{max} approximation?

In order to answer the first question we computed $E_A^{vert\text{-}a}$(LR,neq) energies using two triads of functionals relying on the same correlation part but using a GGA, a global hybrid, and a range-separated hybrid as exchange counterpart, respectively. More precisely, we considered, on one hand, BLYP, B3LYP, and CAM-B3LYP and, on the other, PBE, PBE0, and LC-PBE. For these two trios, all possible geometry/vertical TD combinations have been performed for a subset of molecules (systems **I**−**X**). The full results can be found in Table S-XX, Supporting Information. As expected, increasing the amount of *exact* exchange used during the TD-DFT calculations increases the transition energy, irrespective of the geometry optimization method. The mean variation is +0.29 eV when going from BLYP to B3LYP and +0.27 eV when using CAM-B3LYP instead of B3LYP.[156] The selected PBE triad that implies larger variations of HF-like exchange displays stronger changes: +0.36 eV from PBE to PBE0 and +0.47 eV from PBE0 to LC-PBE.[156] Certainly more surprising is the impact of the geometry. One could foresee that optimizing the geometrical parameters with hybrid functionals instead of GGA would provide more localized structures, e.g., a larger and more realistic bond length alternation[157−159] and hence larger transition energies, but the amplitude of this effect is in fact quite large. Indeed, going from BLYP to B3LYP (PBE to PBE0) geometries and using the same TD protocol induces an average shift of +0.08 (+0.09) eV.[160] Replacing global by range-separated hybrid structures also produces pronounced effects: +0.06 (+0.13) eV for B3LYP to CAM-B3LYP (PBE0 to LC-PBE).[160] Consequently, benchmarking TD-CAM-B3LYP on a BLYP structure implies an average −0.14 eV deviation compared to the fully consistent CAM-B3LYP approach. Moreover, depending on the selected dye, this variation ranges from −0.08 (**II**) to −0.22 eV (**III** and **VII**), so that application of a constant correction would not be satisfying. Clearly, selection of the GS geometries is not such an "innocent" decision when benchmarking TD functionals. Consequently, the results of section 3.2 correspond to a single-pot geometry/spectra assessment of the pros and cons of hybrid functionals, whereas the results of our previous vertical benchmarks[49] are only valuable if PBE0 (or a very similar) geometries are used. This also partly explains why functionals encompassing a large share of *exact* exchange were found as most effective within

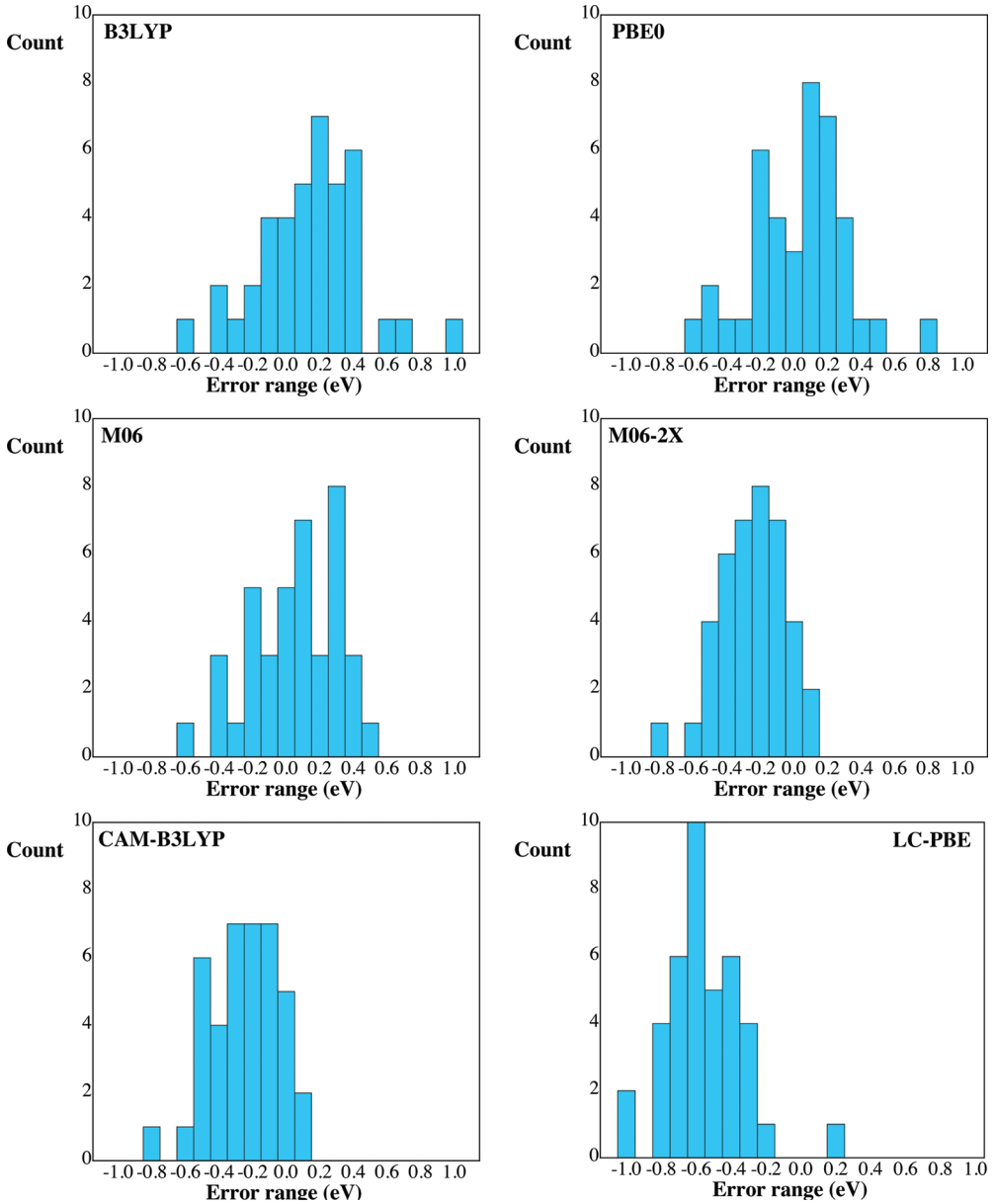

Figure 3. Histograms of the errors computed between the TBE and the experimental 0−0 energies for the six functionals.

Table 5. MAE and MSE (in brackets, in eV) Obtained for Key Parameters by Comparing Gas-Phase and PCM Results [MSE = PCM-gas][a]

method	$E^{\text{vert-a}}$ (LR,eq)	$E^{\text{vert-a}}$ (LR,neq)	$E^{\text{vert-a}}$ (cLR,neq)	$E^{\text{vert-f}}$ (cLR,neq)	ΔE^{ZPVE} (LR,eq)	E^{0-0} (LR,eq)
B3LYP	0.18 (−0.18)	0.12 (−0.12)	0.06 (−0.06)	0.12 (−0.03)	0.01 (−0.01)	0.16 (−0.16)
PBE0	0.18 (−0.18)	0.12 (−0.12)	0.05 (−0.05)	0.09 (−0.01)	0.01 (−0.01)	0.17 (−0.17)
M06	0.18 (−0.18)	0.12 (−0.12)	0.05 (−0.05)	0.07 (−0.02)	0.01 (−0.01)	0.17 (−0.17)
M06-2X	0.19 (−0.19)	0.13 (−0.13)	0.06 (−0.06)	0.10 (−0.03)	0.01 (−0.01)	0.19 (−0.19)
CAM-B3LYP	0.19 (−0.19)	0.13 (−0.13)	0.06 (−0.05)	0.08 (−0.05)	0.01 (−0.01)	0.19 (−0.19)
LC-PBE	0.21 (−0.21)	0.14 (−0.14)	0.06 (−0.06)	0.07 (−0.07)	0.01 (−0.01)	0.21 (−0.21)
all	0.19 (−0.19)	0.13 (−0.13)	0.06 (−0.06)	0.09 (−0.03)	0.01 (−0.01)	0.18 (−0.18)

[a]These values have been obtained with the A basis set on molecules **I**−**X** of Scheme 1.

Grimme's protocol:[51] selection of PBE geometries partially favored a large HF ratio during TD-DFT calculations. Of course, this effect could be mitigated by other corrections used in ref 51.

For the same dyes (**I**−**X**) we performed gas-phase calculations (results in Table S-XXI, Supporting Information) in order to compare them to the values obtained in solution. The main statistical results can be found in Table 5. Of course, the computed solvatochromic shifts strongly depend on the polarity of the solvent, but the chosen compounds represent a diverse panel with six apolar cases and four strongly polar solvents. Nevertheless, for the sake of compactness, we

considered only average effects. Since the ES are generally more polar, that is, more stabilized by the environment than the corresponding GS, inclusion of solvent effects typically leads to a bathochromic shift. As can be seen in Table 5, the average solvatochromic effects are relatively independent of the selected xc functional, though one notices a modest growth of the shifts when functionals including a larger amount of *exact* exchange are applied. The ΔE^{ZPVE} is almost unaffected by the solvent (0.01 eV), so that a gas-phase estimate would not be problematic. For the vertical absorption energies, the cLR PCM model predicts an average shift of ca. −0.05 eV, a small but non-negligible fluctuation given the scale of the errors (see section 3.2). Quite surprisingly, the LR PCM model is quite unsatisfying for $E^{vert\text{-}a}$: it overestimates the solvatochromic shift by a factor of 2 (or 3 if the equilibrium limit is incorrectly used). The emission energies behave similarly to their absorption counterparts, but the solvatochromic effects are more molecule dependent. This outcome is related to the stronger influence of the solvent on ES than GS structures. For instance, for coumarin (**III**), the PCM-TD-DFT ES structure is planar whereas its gas-phase analogue is kinked (see also ref 129), inducing significant discrepancies in computed fluorescence wavelengths. The E^{0-0}(LR,eq) solvatochromism parallels the $E^{vert\text{-}a}$(LR,eq) solvatochromism: correcting gas-phase adiabatic energies by PCM effects calculated on vertical absorption energies is a reasonable first-order approximation. In short, solvent effects are not huge on average, but neglecting them could have serious consequences for several molecules.

Table 6. Statistical Analysis Obtained from the Comparison of the Theoretical Vertical Energies (eq 17) with the Experimental λ^{max} of Table 1 (in eV)

method	MSE	MAE	rms	SD	*R*	max(+)	max(−)
B3LYP	−0.06	0.25	0.30	0.12	0.90	0.63	−0.61
PBE0	0.05	0.22	0.28	0.11	0.92	0.71	−0.41
M06	0.01	0.24	0.28	0.11	0.91	0.69	−0.38
M06−2X	0.36	0.36	0.40	0.15	0.97	0.82	0.04
CAM-B3LYP	0.35	0.35	0.39	0.15	0.97	0.85	0.01
LC-PBE	0.75	0.75	0.77	0.29	0.97	1.11	−0.02

In Table 6 we present a statistical analysis of the errors obtained when comparing the theoretical best estimate of vertical absorption computed as

$$E_A^{vert\text{-}a}(\text{TBE}) = E_A^{vert\text{-}a}(\text{cLR, neq}) + [E_C^{vert\text{-}a}(\text{LR, neq}) - E_A^{vert\text{-}a}(\text{LR, neq})] \quad (17)$$

to the experimental λ_{max} listed in Table 1. Note that when a multipeak (vibronic) structure is present, the experimental λ_{max} has been selected as the band corresponding to the most intense absorption. For the B3LYP, PBE0, and M06 trio, the statistical data of Table 6 are completely similar to those of Table 4, e.g., the MAE obtained with PBE0 remains 0.22 eV and the linear correlation coefficient listed in these two tables is within 0.03 of each other. Note that the PBE0 MAE computed within the same vertical approximation but for a much larger set of molecules was also 0.22 eV,[49] hinting that the selected 40 dyes constitute a representative panel. The fact that the vertical versus λ_{max} and 0−0 versus the abs−fluo crossing point strategies provide the same conclusions for the these three "classical" hybrids is related to an error compensation for the former scheme:[49] vertical energies are larger than their 0−0 counterpart by an average amount that is close to the experimental difference between, on one hand, the measured absorption and fluorescence crossing point and, on the other, the maximum of the absorption band. However, this "lucky" compensation is strongly molecule dependent: we do not advocate systematic use of the vertical approximation. More importantly, the error compensation phenomenon loses its balance for both M06-2X and CAM-B3LYP, which yield less satisfying results within the vertical approximation, with MAE close to 0.35 eV in Table 6, ca. 0.10 eV larger than their 0−0 counterparts reported in Table 4. In other words, hybrids incorporating a large share of HF exchange are "disadvantaged" by the vertical approach. In that sense, the present work reconciles previous conflicting conclusions.[49−51,53] Indeed, we show that while PBE0 average errors are almost unaffected by the selected benchmark strategy, M06-2X's and CAM-B3LYP's efficiencies become apparent only when the structures of the ES are consistently considered.

4. CONCLUSIONS

Using a panel of 40 conjugated molecules, we benchmarked six functionals (B3LYP, PBE0, M06, M06-2X, CAM-B3LYP, and LC-PBE) in the framework of the simulation of optical 0−0 energies. Both basis set and solvent effects have been carefully simulated in order to obtain theoretical best estimates that can be straightforwardly compared to the experimental absorption/emission crossing points. For each functional and molecule, fully consistent calculations (all structures, vibrational spectra, and transition energies computed with the selected approach) have been achieved. Overall, the functionals providing the smallest mean absolute error are PBE0 and M06, with an average deviation of ca. 0.22 eV. Unfortunately, this success is at the price of a rather limited consistency (R = 0.89), which might be partly explained by the qualitatively incorrect excited-state geometries obtained for specific molecules using PBE0 (and other similar hybrids). Both M06-2X and CAM-B3LYP provide very similar results for the majority of dyes; they avoid the obvious qualitative failures and allow one to improve the experiment/theory correlation (R = 0.95) without significantly deteriorating the mean deviation (MAE of 0.25 eV). Therefore, these functionals should be preferred when simulating 0−0 energies, though PBE0 and M06 have a clear edge if one relies on the (faster) vertical approximation that does not require optimization of the excited-state geometries. Furthermore, the present investigation provided several extra conclusions.

1 Variation of the zero-point vibrational energies from the ground to the excited states is nearly basis set independent, is almost unaffected by the environment, is slightly tuned by the functional choice but significantly depends on the molecule under study.
2 Basis set effects are mainly related to vertical contributions but remain relatively small once a basis set containing both polarization and diffuse functions is selected.
3 Solvent effects cannot be neglected, and use of the linear-response PCM approximation is insufficient to quantitatively capture solvatochromism, even in the case of the absorption spectra.

4 The selected structural optimization method significantly affects TD-DFT vertical transition energies and, consequently, the results of TD-DFT benchmarks.

The data collected in the Supporting Information, that is the CAM-B3LYP/6-31+G(d) geometries and ZPVE, might also be helpful to test new functionals by performing relatively quick calculations: one "only" needs to determine the adiabatic energies in the eq and neq limits, a task that can be done by vertical TD-DFT calculations performed on the GS and ES structures.

■ ASSOCIATED CONTENT

Supporting Information

Tables with full list of "raw" computed data (absorption, fluorescence, and adiabatic energies with the six functionals and different solvent models); alternative options to compute the TBE and error patterns obtained with these alternatives; cross geometry/spectra vertical energies for molecules **I**–**X** and gas-phase vertical and adiabatic data for the same set; Cartesian coordinates for all GS and ES at the CAM-B3LYP/6-31+G(d) level. This material is available free of charge via the Internet at http://pubs.acs.org.

■ AUTHOR INFORMATION

Corresponding Author

*E-mail: Denis.Jacquemin@univ-nantes.fr (D.J.); carlo-adamo@chimie-paristech.fr (C. A.); bene@dcci.unipi.it (B.M.).

Notes

The authors declare no competing financial interest.

■ ACKNOWLEDGMENTS

The authors thank Dr. I. Ciofini for fruitful discussions. D.J. acknowledges the European Research Council (ERC) and *Région des Pays de la Loire* for financial support in the framework of a Starting Grant (Marches-278845) and a *recrutement sur poste stratégique*, respectively. B.M. acknowledges the European Research Council (ERC) for financial support in the framework of the Starting Grant (EnLight -277755). This research used resources of the (1) GENCI-CINES/IDRIS (Grants c2011085117 and c2012085117), (2) CCIPL (*Centre de Calcul Intensif des Pays de Loire*), and (3) Interuniversity Scientific Computing Facility located at the University of Namur, Belgium, which is supported by the F.R.S.-FNRS under convention no. 2.4617.07. The authors are indebted to the COST program CODECS and its members for support and many helpful discussions, respectively.

■ REFERENCES

(1) Becke, A. D. *J. Chem. Phys.* **1993**, *98*, 1372–1377.
(2) Becke, A. D. *J. Chem. Phys.* **1993**, *98*, 5648–5652.
(3) Perdew, J. P.; Ernzerhof, M.; Burke, K. *J. Chem. Phys.* **1996**, *105*, 9982–9985.
(4) Adamo, C.; Barone, V. *J. Chem. Phys.* **1999**, *110*, 6158–6170.
(5) Ernzerhof, M.; Scuseria, G. E. *J. Chem. Phys.* **1999**, *110*, 5029–5036.
(6) Zhao, Y.; Schultz, N. E.; Truhlar, D. G. *J. Chem. Phys.* **2005**, *123*, 161103.
(7) Zhao, Y.; Truhlar, D. G. *Acc. Chem. Res.* **2008**, *41*, 157–167.
(8) Zhao, Y.; Truhlar, D. G. *Theor. Chem. Acc.* **2008**, *120*, 215–241.
(9) Boese, A. D.; Martin, J. M. L. *J. Chem. Phys.* **2004**, *121*, 3405–3416.
(10) Savin, A. In *Recent Developments and Applications of Modern Density Functional Theory*; Seminario, J. M., Ed.; Elsevier: Amsterdam, 1996; Chapter 9, pp 327–354.
(11) Iikura, H.; Tsuneda, T.; Yanai, T.; Hirao, K. *J. Chem. Phys.* **2001**, *115*, 3540–3544.
(12) Yanai, T.; Tew, D. P.; Handy, N. C. *Chem. Phys. Lett.* **2004**, *393*, 51–56.
(13) Vydrov, O. A.; Scuseria, G. E. *J. Chem. Phys.* **2006**, *125*, 234109.
(14) Chai, J. D.; Head-Gordon, M. *J. Chem. Phys.* **2008**, *128*, 084106.
(15) Baer, R.; Livshits, E.; Salzner, U. *Annu. Rev. Phys. Chem.* **2010**, *61*, 85–109.
(16) Grimme, S. *J. Chem. Phys.* **2006**, *124*, 034108.
(17) Grimme, S.; Neese, F. *J. Chem. Phys.* **2007**, *127*, 154116.
(18) Toulouse, J.; Sharkas, K.; Brémond, E.; Adamo, C. *J. Chem. Phys.* **2011**, *135*, 101102.
(19) Sharkas, K.; Toulouse, J.; Savin, A. *J. Chem. Phys.* **2011**, *134*, 064113.
(20) Fromager, E. *J. Chem. Phys.* **2011**, *135*, 244106.
(21) Brémond, E.; Adamo, C. *J. Chem. Phys.* **2011**, *135*, 024106.
(22) Grimme, S. *J. Comput. Chem.* **2004**, *25*, 1463–1476.
(23) Johnson, E. R.; Becke, A. D. *J. Chem. Phys.* **2006**, *124*, 174104.
(24) Grimme, S. *J. Comput. Chem.* **2006**, *27*, 1787–1799.
(25) Chai, J. D.; Head-Gordon, M. *Phys. Chem. Chem. Phys.* **2008**, *10*, 6615–6620.
(26) Grimme, S.; Antony, J.; Ehrlich, S.; Krieg, H. *J. Chem. Phys.* **2010**, *132*, 154104.
(27) Runge, E.; Gross, E. K. U. *Phys. Rev. Lett.* **1984**, *52*, 997–1000.
(28) Casida, M. E. In *Time-Dependent Density-Functional Response Theory for Molecules*; Chong, D. P., Ed.; World Scientific: Singapore, 1995; Vol. *1*, pp 155–192.
(29) Stratmann, R. E.; Scuseria, G. E.; Frisch, M. J. *J. Chem. Phys.* **1998**, *109*, 8218–8224.
(30) Dreuw, A.; Head-Gordon, M. *Chem. Rev.* **2005**, *105*, 4009–4037.
(31) Casida, M. E. *J. Mol. Struct. (THEOCHEM)* **2009**, *914*, 3–18.
(32) Jacquemin, D.; Mennucci, B.; Adamo, C. *Phys. Chem. Chem. Phys.* **2011**, *13*, 16987–16998.
(33) Fabian, J. *Theor. Chem. Acc.* **2001**, *106*, 199–217.
(34) Matsuura, M.; Sato, H.; Sotoyama, W.; Takahashi, A.; Sakurai, M. *J. Mol. Struct. (THEOCHEM)* **2008**, *860*, 119–127.
(35) Silva-Junior, M. R.; Thiel, W. *J. Chem. Theory Comput.* **2010**, *6*, 1546–1564.
(36) Stanton, J. F.; Bartlett, R. J. *J. Chem. Phys.* **1993**, *98*, 7029–7039.
(37) McDouall, J. J.; Peasley, K.; Robb, M. A. *Chem. Phys. Lett.* **1988**, *148*, 183–189.
(38) Nakatsuji, H. *J. Chem. Phys.* **1991**, *94*, 6716–6727.
(39) Nakatsuji, H.; Ehara, M. *J. Chem. Phys.* **1993**, *98*, 7179–7184.
(40) Buenker, R. J.; Peyerimhoff, S. D.; Butscher, W. *Mol. Phys.* **1978**, *35*, 771–791.
(41) Cossi, M.; Barone, V. *J. Chem. Phys.* **2001**, *115*, 4708–4717.
(42) Caricato, M.; Mennucci, J.; Tomasi, B.; Ingrosso, F.; Cammi, R.; Corni, S.; Scalmani, G. *J. Chem. Phys.* **2006**, *124*, 124520.
(43) Scalmani, G.; Frisch, M. J.; Mennucci, B.; Tomasi, J.; Cammi, R.; Barone, V. *J. Chem. Phys.* **2006**, *124*, 094107.
(44) Improta, R.; Barone, V.; Scalmani, G.; Frisch, M. J. *J. Chem. Phys.* **2006**, *125*, 054103.
(45) Marenich, A. V.; Cramer, C. J.; Truhlar, D. G.; Guido, C. G.; Mennucci, B.; Scalmani, G.; Frisch, M. J. *Chem. Sci* **2011**, *2*, 2143–2161.
(46) Wiggins, P.; Gareth Williams, J. A.; Tozer, D. J. *J. Chem. Phys.* **2009**, *131*, 091101.
(47) Guido, C. A.; Mennucci, B.; Jacquemin, D.; Adamo, C. *Phys. Chem. Chem. Phys.* **2010**, *12*, 8016–8023.
(48) Plötner, J.; Tozer, D. J.; Dreuw, A. *J. Chem. Theory Comput.* **2010**, *6*, 2315–2324.
(49) Jacquemin, D.; Wathelet, V.; Perpète, E. A.; Adamo, C. *J. Chem. Theory Comput.* **2009**, *5*, 2420–2435.
(50) Goerigk, L.; Moellmann, J.; Grimme, S. *Phys. Chem. Chem. Phys.* **2009**, *11*, 4611–4620.

(51) Goerigk, L.; Grimme, S. *J. Chem. Phys.* **2010**, *132*, 184103.
(52) Jacquemin, D.; Perpète, E. A.; Ciofini, I.; Adamo, C. *J. Chem. Theory Comput.* **2010**, *6*, 1532−1537.
(53) Jacquemin, D.; Perpète, E. A.; Ciofini, I.; Adamo, C.; Valero, R.; Zhao, Y.; Truhlar, D. G. *J. Chem. Theory Comput.* **2010**, *6*, 2071−2085.
(54) Caricato, M.; Trucks, G. W.; Frisch, M. J.; Wiberg, K. B. *J. Chem. Theory Comput.* **2010**, *6*, 370−383.
(55) Caricato, M.; Trucks, G. W.; Frisch, M. J.; Wiberg, K. B. *J. Chem. Theory Comput.* **2011**, *7*, 456−166.
(56) Jacquemin, D.; Perpète, E. A.; Ciofini, I.; Adamo, C. *Theor. Chem. Acc.* **2011**, *128*, 127−136.
(57) Sears, J. S.; Koerzdoerfer, T.; Zhang, C. R.; Brédas, J. L. *J. Chem. Phys.* **2011**, *135*, 151103.
(58) Send, R.; Kühn, M.; Furche, F. *J. Chem. Theory Comput.* **2011**, *7*, 2376−2386.
(59) Jacquemin, D.; Brémond, E.; Planchat, A.; Ciofini, I.; Adamo, C. *J. Chem. Theory Comput.* **2011**, *174*, 1882−1892.
(60) Goerigk, L.; Grimme, S. *J. Chem. Theory Comput.* **2011**, *7*, 3272−3277.
(61) Peach, M. J. G.; Williamson, M. J.; Tozer, D. J. *J. Chem. Theory Comput.* **2011**, *7*, 3578−3585.
(62) Della Sala, F.; Fabiano, E. *Chem. Phys.* **2011**, *391*, 19−26.
(63) Huix-Rotllant, M.; Ipatov, A.; Rubio, A.; Casida, M. E. *Chem. Phys.* **2011**, *391*, 120−129.
(64) Leang, S. S.; Zahariev, F.; Gordon, M. S. *J. Chem. Phys.* **2012**, *136*, 104101.
(65) Jacquemin, D.; Adamo, C. *Int. J. Quantum Chem.* **2012**, *112*, 2135−2141.
(66) Schreiber, M.; Silva-Junior, M. R.; Sauer, S. P. A.; Thiel, W. *J. Chem. Phys.* **2008**, *128*, 134110.
(67) Silva-Junior, M. R.; Schreiber, M.; Sauer, S. P. A.; Thiel, W. *J. Chem. Phys.* **2008**, *129*, 104103.
(68) Sauer, S. P. A.; Schreiber, M.; Silva-Junior, M. R.; Thiel, W. *J. Chem. Theory Comput.* **2009**, *5*, 555−564.
(69) Silva-Junior, M. R.; Sauer, S. P. A.; Schreiber, M.; Thiel, W. *Mol. Phys.* **2010**, *108*, 453−465.
(70) Silva-Junior, M. R.; Schreiber, M.; Sauer, S. P. A.; Thiel, W. *J. Chem. Phys.* **2010**, *133*, 174318.
(71) Send, R.; Valsson, O.; Filippi, C. *J. Chem. Theory Comput.* **2011**, *7*, 444−455.
(72) Jacquemin, D.; Zhao, Y.; Valero, R.; Adamo, C.; Ciofini, I.; Truhlar, D. G. *J. Chem. Theory Comput.* **2012**, *8*, 1255−1259.
(73) Tomasi, J.; Mennucci, B.; Cammi, R. *Chem. Rev.* **2005**, *105*, 2999−3094.
(74) Frisch, M. J.; Trucks, G. W.; Schlegel, H. B.; Scuseria, G. E.; Robb, M. A.; Cheeseman, J. R.; Scalmani, G.; Barone, V.; Mennucci, B.; Petersson, G. A.; Nakatsuji, H.; Caricato, M.; Li, X.; Hratchian, H. P.; Izmaylov, A. F.; Bloino, J.; Zheng, G.; Sonnenberg, J. L.; Hada, M.; Ehara, M.; Toyota, K.; Fukuda, R.; Hasegawa, J.; Ishida, M.; Nakajima, T.; Honda, Y.; Kitao, O.; Nakai, H.; Vreven, T.; Montgomery, J. A., Jr.; Peralta, J. E.; Ogliaro, F.; Bearpark, M.; Heyd, J. J.; Brothers, E.; Kudin, K. N.; Staroverov, V. N.; Kobayashi, R.; Normand, J.; Raghavachari, K.; Rendell, A.; Burant, J. C.; Iyengar, S. S.; Tomasi, J.; Cossi, M.; Rega, N.; Millam, J. M.; Klene, M.; Knox, J. E.; Cross, J. B.; Bakken, V.; Adamo, C.; Jaramillo, J.; Gomperts, R.; Stratmann, R. E.; Yazyev, O.; Austin, A. J.; Cammi, R.; Pomelli, C.; Ochterski, J. W.; Martin, R. L.; Morokuma, K.; Zakrzewski, V. G.; Voth, G. A.; Salvador, P.; Dannenberg, J. J.; Dapprich, S.; Daniels, A. D.; Farkas, O.; Foresman, J. B.; Ortiz, J. V.; Cioslowski, J.; Fox, D. J. *Gaussian 09*, Revision A.02; Gaussian Inc.: Wallingford, CT, 2009.
(75) Stephens, P. J.; Devlin, F. J.; Chabalowski, C. F.; Frisch, M. J. *J. Phys. Chem.* **1994**, *98*, 11623−11627.
(76) Song, J. W.; Hirosawa, T.; Tsuneda, T.; Hirao, K. *J. Chem. Phys.* **2007**, *126*, 154105.
(77) Peach, M. J. G.; Benfield, P.; Helgaker, T.; Tozer, D. J. *J. Chem. Phys.* **2008**, *128*, 044118.
(78) Jacquemin, D.; Perpète, E. A.; Scalmani, G.; Frisch, M. J.; Kobayashi, R.; Adamo, C. *J. Chem. Phys.* **2007**, *126*, 144105.
(79) Jacquemin, D.; Perpète, E. A.; Scuseria, G. E.; Ciofini, I.; Adamo, C. *J. Chem. Theory Comput.* **2008**, *4*, 123−135.
(80) Mardirossian, N.; Parkhill, J. A.; Head-Gordon, M. *Phys. Chem. Chem. Phys.* **2011**, *13*, 19325−19337.
(81) Hay, P. J.; Wadt, W. R. *J. Chem. Phys.* **1985**, *82*, 284.
(82) Hay, P. J.; Wadt, W. R. *J. Chem. Phys.* **1985**, *85*, 299.
(83) Petit, L.; Maldivi, P.; Adamo, C. *J. Chem. Theory Comput.* **2005**, *1*, 953−962.
(84) Wheeler, S. E.; Houk, K. N. *J. Chem. Theory Comput.* **2010**, *6*, 395−404.
(85) Li, X.; Frisch, M. J. *J. Chem. Theory Comput.* **2006**, *2*, 835−839.
(86) van Caillie, C.; Amos, R. D. *Chem. Phys. Lett.* **1999**, *308*, 249−255.
(87) van Caillie, C.; Amos, R. D. *Chem. Phys. Lett.* **2000**, *317*, 159−164.
(88) Furche, F.; Ahlrichs, R. *J. Chem. Phys.* **2002**, *117*, 7433−7447.
(89) Improta, R.; Barone, V. *J. Mol. Struct. (THEOCHEM)* **2009**, *914*, 87−93.
(90) Avila Ferrer, F. J.; Improta, R.; Santoro, F.; Barone, V. *Phys. Chem. Chem. Phys.* **2011**, *13*, 17007−17012.
(91) Berlman, I. B. *Handbook of fluorescence spectra of aromatic molecules*, 2nd ed.; Academic Press: New York, 1971.
(92) Pavlopoulos, T. G. *J. Appl. Phys.* **1986**, *60*, 4028−4030.
(93) Kreller, D. I.; Kamat, P. V. *J. Phys. Chem.* **1991**, *95*, 4406−4410.
(94) Heldt, J. R.; Helds, J.; Ston, M.; Diehl, H. A. *Spectrochim. Acta A* **1995**, *51*, 1549−1563.
(95) Bishop, S.; Beeby, A.; Parker, A.; Foley, M.; Phillips, D. *J. Photochem. Photobiol. A: Chem.* **1995**, *90*, 39−44.
(96) Dutta, A. K.; Kamada, K.; Ohta, K. *J. Photochem. Photobiol. A: Chem.* **1996**, *93*, 57−64.
(97) Du, H.; Fuh, R. A.; Li, J.; Corkan, A.; Lindsey, J. S. *Photochem. Photobiol.* **1998**, *68*, 141−142. Spectra available at http://omlc.ogi.edu/spectra/PhotochemCAD/ and at http://www.fluorophores.tugraz.at/.
(98) Lewis, F. D.; Kalgutkar, R. S.; Yang, J.-S. *J. Am. Chem. Soc.* **1999**, *121*, 12045−12053.
(99) Mühlpfordt, A.; Schanz, R.; Ernsting, N. P.; Farztdinov, V.; Grimme, S. *Phys. Chem. Chem. Phys.* **1999**, *1*, 3209−3218.
(100) van Veldhoven, E.; Zhang, H.; Glasbeek, M. *J. Phys. Chem. A* **2001**, *105*, 1687−1692.
(101) Ichino, Y.; Ni, J. P.; Ueda, Y.; Wang, D. K. *Synth. Met.* **2001**, *116*, 223−227.
(102) Belletete, M.; Morin, J. F.; Beaupre, S.; Ranger, M.; Leclerc, M.; Durocher, G. *Macromolecules* **2001**, *34*, 2288−2297.
(103) Connors, R. E.; Ucak-Astarlioglu, M. G. *J. Phys. Chem. A* **2003**, *107*, 7684−7691.
(104) Cheng, Y. M.; Yeh, Y. S.; Ho, M. L.; Chou, P. T.; Chen, P. S.; Chi, Y. *Inorg. Chem.* **2005**, *44*, 4594−4603.
(105) Seixas de Melo, J. S.; Rondao, R.; Burrows, H. D.; Melo, M. J.; Navaratman, S.; Edge, R.; Voss, G. *ChemPhysChem* **2006**, *7*, 2303−2311.
(106) Clarke, T. C.; Gordon, K. C.; Kwok, W. M.; Phillips, D. L.; Officer, D. L. *J. Phys. Chem. A* **2006**, *110*, 7696−7702.
(107) Barbarella, G.; Zambianchi, M.; Ventola, A.; Fabiano, E.; Della Sala, F.; Gigli, G.; Anni, M.; Bolognesi, A.; Polito, L.; Naldi, M.; Capobianco, M. *Biooconjugate Chem.* **2006**, *17*, 58−67.
(108) Magalhaes, J. L.; Pereira, R. V.; Triboni, E. R.; Berci Filho, P.; Gehlen, M. H.; Nart, F. C. *J. Photochem. Photobiol. A: Chem.* **2006**, *183*, 165−170.
(109) Yoshino, J.; Kano, N.; Kawashima, T. *Chem. Commun.* **2007**, 559−561.
(110) Donyagina, V.; Shimizu, S.; Kobayashi, N.; Lukyanets, E. A. *Tetrahderon Lett.* **2008**, *48*, 6152−6154.
(111) Tram, K.; Yan, H.; Jenkins, H. A.; Vassiliev, S.; Bruce, D. *Dyes Pigm.* **2009**, *82*, 392−395.
(112) Ma, Y.; Hao, R.; Shao, G.; Wang, Y. *J. Phys. Chem. A* **2009**, *113*, 5066−5072.
(113) Abdel-Halim, S. T.; Awad, M. K. *J. Mol. Struct.* **2009**, *920*, 332−341.

(114) Sajadi, M.; Obernhuber, T.; Kovalenko, S. A.; Mosquera, M.; Dick, B.; Ernsting, N. P. *J. Phys. Chem. A* **2009**, *113*, 44−55.
(115) Henssler, J. T.; Zhang, X.; Matzger, A. J. *J. Org. Chem.* **2009**, *74*, 9112−9119.
(116) Younes, A. H.; Zhang, L.; Clark, R. J.; Zhu, L. *J. Org. Chem.* **2009**, *74*, 8761−8772.
(117) Gryko, D. T.; Piechowska, J.; Galzeowski. *J. Org. Chem.* **2010**, *75*, 1297−1300.
(118) Zakerhamidi, M. S.; Ghanadzadeh, A.; Moghadam, M. *Spectrochim. Acta A* **2011**, *79*, 74−81.
(119) Pawlowska, Z.; Lietard, A.; Aloise, S.; Sliwa, M.; Idrissi, A.; Poizat, O.; Buntinx, G.; Delbaere, S.; Perrier, A.; Maurel, F.; Jacques, F.; Abe, J. *Phys. Chem. Chem. Phys.* **2011**, *13*, 13185−13195.
(120) Bruckstummer, H.; Weissenstein, A.; Bialas, D.; Wurthner, F. *J. Org. Chem.* **2011**, *76*, 2426−2432.
(121) Shanker, N.; Dilek, O.; Mukherjee, T.; McGee, D. W.; Bane, S. L. *J. Fluoresc.* **2011**, *21*, 2173−2184.
(122) Erten-Ela, S.; Ozcelik, S.; Eren, E. *J. Fluoresc.* **2011**, *21*, 1565−1573.
(123) Warnan, J.; Favereau, L.; Pellegrin, Y.; Blart, E.; Jacquemin, D.; Odobel, F. *J. Photochem. Photobiol. A: Chem.* **2011**, *226*, 9−15.
(124) Georgiev, N. I.; Sakr, A. R.; Bojinov, V. B. *Dyes Pigm.* **2011**, *91*, 332−339.
(125) Georgieva, I.; Trendafilova, N.; Aquino, A.; Lischka, H. *J. Phys. Chem. A* **2005**, *109*, 11860−11869.
(126) Jacquemin, D.; Perpète, E. A.; Scalmani, G.; Frisch, M. J.; Assfeld, X.; Ciofini, I.; Adamo, C. *J. Chem. Phys.* **2006**, *125*, 164324.
(127) Ingrosso, F.; Ladanyi, B. M.; Mennucci, B.; Scalmani, G. *J. Phys. Chem. B* **2006**, *110*, 4953−4962.
(128) Improta, R.; Barone, V.; Santoro, F. *Angew. Chem., Int. Ed. Engl.* **2007**, *46*, 405−408.
(129) Jacquemin, D.; Perpète, E. A.; Assfeld, X.; Scalmani, G.; Frisch, M. J.; Adamo, C. *Chem. Phys. Lett.* **2007**, *438*, 208−212.
(130) Wong, B. M.; Cordaro, J. G. *J. Chem. Phys.* **2008**, *129*, 214703.
(131) Sanchez-de Armas, R.; San Miguel, M. A.; Oviedo, J.; Sanz, J. F. *Phys. Chem. Chem. Phys.* **2012**, *14*, 225−233.
(132) Jacquemin, D.; Perpète, E. A.; Scalmani, G.; Frisch, M. J.; Ciofini, I.; Adamo, C. *Chem. Phys. Lett.* **2007**, *448*, 3−6.
(133) Miao, L.; Yao, Y.; Yang, F.; Wang, Z.; Li, W.; Hu, J. *J. Mol. Struct. (THEOCHEM)* **2008**, *865*, 79−87.
(134) Kucheryavy, P.; Li, G.; Vyas, S.; Hadad, C.; Glusac, K. D. *J. Phys. Chem. A* **2009**, *113*, 6453−6461.
(135) Jacquemin, D.; Perpete, E. A.; Scalmani, G.; Ciofini, I.; Peltier, C.; Adamo, C. *Chem. Phys.* **2010**, *372*, 61−66.
(136) Cheshmedzhieva, D.; Ivanova, P.; Stoyanov, S.; Tasheva, D.; Dimitrova, M.; Ivanov, I.; Ilieva, S. *Phys. Chem. Chem. Phys.* **2011**, *13*, 18530−18538.
(137) Quartarolo, A. D.; Russo, N.; Sicilia, E. *Chem.—Eur. J.* **2006**, *12*, 6797−6803.
(138) Loudet, A.; Burgess, K. *Chem. Rev.* **2007**, *107*, 4891−4932.
(139) Le Guennic, B.; Maury, O.; Jacquemin, D. *Phys. Chem. Chem. Phys.* **2012**, *14*, 157−164.
(140) Schreiber, M.; Bub, V.; Fülscher, M. P. *Phys. Chem. Chem. Phys.* **2001**, *3*, 3906−3912.
(141) Fabian, J. *Dyes Pigm.* **2010**, *84*, 36−53.
(142) Cammi, R.; Mennucci, B. *J. Chem. Phys.* **1999**, *110*, 9877−9886.
(143) We emphasize that in Gaussian09 (1) the default for single-point PCM-TD-DFT calculations is (LR,neq), whereas ES optimizations use (LR,eq), i.e., the final transition energy of PCM-TD-DFT force minimization processes is not the noneq fluorescence value (it should be determined separately) and (2) $E^{\text{vert-a}}$(cLR;neq/eq) can be counter-intuitively determined with the G09.A revisions using the STATESPECIFIC keyword, whereas $E^{\text{vert-a}}$(SS;neq/eq) are obtained with the EXTERNALITERATION keyword. In subsequent revisions, both keywords yield the state-specific values. As said above, $E^{\text{vert-a}}$(cLR;neq/eq) cannot be obtained with the G09.A revision, and they have been obtained with a locally modified version of the same code.
(144) Hehre, W.; Ditchfield, R.; Pople, J. A. *J. Chem. Phys.* **1972**, *56*, 2257−2261.
(145) Hariharan, P. C.; Pople, J. A. *Theor. Chim. Acta* **1973**, *28*, 213−222.
(146) Krishnan, R.; Binkley, J. S.; Seeger, R.; Pople, J. A. *J. Chem. Phys.* **1980**, *72*, 650−654.
(147) Dunning, T. H. *J. Chem. Phys.* **1989**, *90*, 1007−1023.
(148) Kendall, R. A.; Dunning, T. H.; Harisson, R. J. *J. Chem. Phys.* **1992**, *96*, 6796−6806.
(149) Woon, D.; Dunning, T. H. *J. Chem. Phys.* **1994**, *100*, 2975−2988.
(150) Jensen, F. *J. Chem. Phys.* **2001**, *115*, 9113.
(151) Jensen, F. *J. Chem. Phys.* **2002**, *116*, 7372.
(152) Jensen, F. *J. Chem. Phys.* **2002**, *117*, 9234.
(153) These values have been obtained by 4.356 + (4.904 − 4.946) and 4.479 + (5.171 − 5.204) eV for PBE0 and CAM-B3LYP, respectively.
(154) Perrier, A.; Aloïse, S.; Pawlowska, Z.; Sliwa, M.; Maurel, F.; Abe, J. *Chem. Phys. Lett.* **2011**, *515*, 42−48.
(155) Aloise, S.; Pawlowska, Z.; Ruckebusch, C.; Sliwa, M.; Dubois, J.; Poizat, O.; Buntinx, G.; Perrier, A.; Maurel, F.; Jacques, P.; Malval, J.-P.; Poisson, L.; Piani, G.; Abe, J. *Phys. Chem. Chem. Phys.* **2012**, *14*, 1945−1956.
(156) Average values over all molecules and geometries of Table S-XVI, Supporting Information.
(157) Peach, M. J. G.; Tellgren, E.; Salek, P.; Helgaker, T.; Tozer, D. J. *J. Phys. Chem. A* **2007**, *111*, 11930−11935.
(158) Sancho-Garcia, J. C.; Perez-Jimenez, A. J. *Phys. Chem. Chem. Phys.* **2007**, *9*, 5874−5879.
(159) Jacquemin, D.; Adamo, C. *J. Chem. Theory Comput.* **2011**, *7*, 369−376.
(160) Average for the 3 TD functionals and 10 molecules investigated.